AN ULTRASTRUCTURAL STUDY OF CROSS-BRIDGE ARRANGEMENT IN THE FROG THIGH MUSCLE THICK FILAMENT

ROBERT W. KENSLER* AND MURRAY STEWART‡§
*Department of Anatomy, The Medical College of Pennsylvania, Philadelphia, Pennsylvania 19129;
‡Medical Research Council Laboratory of Molecular Biology, Cambridge, CB2 2QH, England; and
§Pennsylvania Muscle Institute, University of Pennsylvania Medical School, Philadelphia, Pennsylvania 19104

ABSTRACT We have developed thick filament isolation methods that preserve the relaxed cross-bridge order of frog thick filaments such that the filaments can be analyzed by the convergent techniques of electron microscopy, optical diffraction, and computer image analysis. Images of the filaments shadowed by using either unidirectional shadowing or rotary shadowing show a series of subunits arranged along a series of right-handed near-helical strands that occur every 43 nm axially along the filament arms. Optical filtrations of images of these shadowed filaments show 4–5 subunits per half-turn of the strands, consistent with a three-stranded arrangement of the cross-bridges, thus supporting our earlier results from negative staining and computer-image analysis. The optical diffraction patterns of the shadowed filaments show a departure from the pattern expected for helical symmetry consistent with the presence of cylindrical symmetry and a departure of the cross-bridges from helical symmetry. We also describe a modified negative staining procedure that gives improved delineation of the cross-bridge arrangement. From analysis of micrographs of these negatively stained filament tilted about their long axes, we have computed a preliminary three-dimensional reconstruction of the filament that clearly confirms the three-stranded arrangement of the myosin heads.

INTRODUCTION

Vertebrate striated muscle thick filaments are bipolar macromolecular assemblies of the protein myosin together with small quantities of other accessory proteins (4, 14, 34, 35, 39). The rod-like myosin tails associate to form the filament shaft, while the globular myosin heads lie on the surface of the filament, where in the presence of Ca^{+2} and ATP they form cross-bridges with the adjacent actin thin filaments and produce tension by a sliding filament mechanism (7, 13, 17). An understanding of the detailed molecular structure of the thick filament and of the changes that take place in its structure during contraction is of great significance in understanding how tension is produced at the molecular level during contraction of muscle. Unfortunately, while both the structure of myosin (9, 14, 27) and its aggregation properties (3, 14, 19, 31) have been studied in detail, the precise arrangement of myosin and the accessory proteins in the vertebrate thick filament is still poorly understood. X-ray diffraction studies of frog (10, 11, 15), mammalian (26, 30), and chicken (28) striated muscles have established that the myosin heads in relaxed muscle are arranged nearly helically with an axial repeat of 42.9 nm and with an axial spacing of 14.3 nm between adjacent levels of heads. However, largely because of the loss of the phase information in the patterns combined with the problem of lattice sampling of the diffraction maxima (12, 32), these studies have not allowed a definitive determination of either the number or the precise arrangement of the myosin heads.

As an alternative approach, we (20, 22, 25, 36, 37) and others (2, 5, 42) have in recent years explored the use of electron microscopic and computer image analysis techniques to determine the structure of thick filaments. Procedures have been developed for the isolation of thick filaments from several invertebrate muscles (2, 5, 20, 22, 42) such that the helical ordering of the cross-bridges is preserved, thus allowing electron micrographs of the filaments to be analyzed by the helical diffraction and computer image analysis techniques that have been so powerfully used to analyze other macromolecular assemblies such as decorated actin and viruses (8, 38). Using a similar approach, we (23) have recently shown that frog thick filaments can also be isolated with the cross-bridges in a periodic array. Preliminary computer image analysis of electron micrographs of the negatively stained filaments provided strong evidence for a three-stranded arrangement of the myosin cross-bridges along the filament (23), but did not allow a complete delineation either of the individual myosin heads or their relationship to accessory proteins.

In this paper, we have further examined the structure of the frog thick filament using both unidirectional and rotary shadowing. We present evidence suggesting that the cross-bridge arrangement is perturbed from helical symmetry, and may have cylindrical symmetry. We also describe the appearance of the filament seen using a modified negative staining procedure that provides better delineation of the cross-bridge arrangement. We present a preliminary three-dimensional reconstruction of these filaments based on the analysis of tilt series of a single filament.

MATERIALS AND METHODS

Thick filaments were isolated from whole thigh muscle of the frog, *Rana pipiens*, by a slight modification of the procedure we previously reported (23). 2–5 mm diameter bundles were excised from pithed animals and immediately placed in an EGTA-saline solution containing 0.1 M NaCl, 2 mM EGTA, 1 mM dithiothreitol, 5 mM $MgCl_2$, and 7 mM potassium phosphate buffer (pH 7) at 4°C. After 1–2 h, the muscle bundles were finely teased into smaller diameter bundles (0.2–0.5 mm) with forceps and left overnight in fresh solution of the same composition except for the addition of 2.5 mM ATP. A bundle was then finely minced with a razor blade and homogenized in relaxing solution in which NaCl was replaced with KCl. Homogenization was performed on ice with two 10 s bursts (separated by 30 s) at setting 3 of a Sorvall OmniMixer (Dupont Company, Newtown, CT) using the 5 ml cup. The homogenate was diluted with additional relaxing solution to 15 ml and centrifuged at 3,000 *g* 10 min to pellet the large debris. Separated thick and thin filaments remained in the supernatant and were absorbed onto grids with thin carbon films (5–7 nm) supported by perforated Formvar films.

Negative staining was performed using a tannic acid-uranyl acetate procedure (22). In this procedure, thick filaments adsorbed to the carbon films were rinsed sequentially with eight drops each of relaxing solution, 0.25% tannic acid (Mallinckrodt Ar 1764, Mallinckrodt, Inc., St. Louis, MO) in 0.05 M ammonium acetate, 0.1 M ammonium acetate, and then negatively stained with 1% uranyl acetate. The tannic acid solution was prepared daily as a 0.5% stock which was diluted with an equal volume of 0.1 M ammonium acetate.

For platinum or platinum-carbon shadowing, isolated filaments, adsorbed to standard thickness carbon films on grids, were sequentially rinsed with eight drops each of relaxing solution, 0.1 M ammonium acetate, 1% uranyl acetate, and 10% glycerol. The grids were dried for 30–60 min under vacuum (pressure $\leq 10^{-5}$ Torr) in a Denton DV 502 vacuum evaporator (Denton Vacuum, Cherry Hill, NJ) to remove the glycerol. The uranyl acetate acts to stabilize the filaments against collapse during drying (21, 42) and the glycerol appears to improve the helical ordering of the cross-bridges (42). Shadowing of the filaments with platinum or platinum-carbon was performed as previously described (21) at a shadowing angle of 20–30° and a specimen-to-electrode distance of 15 cm. Rotary shadowing was similarly performed with the specimens rotated at ~60 rpm.

Negatively stained and platinum-shadowed preparations were examined in either a JEOL 100S electron microscope (JEOL USA Electron Optics, Peabody, MA) or a Philips EM300 electron microscope (Philips Electronic Instruments, Mahwah, NJ) with the anticontamination device in operation. Magnification was calibrated using catalase crystals (44) or tropomyosin tactoids (1). For tilt series, micrographs were recorded at 60 kV in a Philips EM400 electron microscope using a rotating stage. Tilt series were recorded at a nominal magnification of 17,000× for tilts of ±45° in 15° steps.

Optical diffraction and optical filtration were performed as previously described (20, 21, 23, 36). Spacings on the diffraction patterns were calculated relative to the spacing (1/14.3 nm^{-1}) of the meridional reflection on the third layer line (43).

For computer image processing, tilt series were assessed by optical diffraction to select filaments that were well preserved and which showed a clear pattern of layer lines similar to that seen in x-ray diffraction patterns of living relaxed frog muscle (15). Selected areas of micrographs were digitized at spacings corresponding to 1 nm intervals on the original specimen and processed essentially as previously described (36, 37). Briefly, the area of interest was selected and, after gaussian edge apodisation, embedded in a 512 × 256 array of zeros. The Fourier transform of this array was computed and layer line data extracted for the equator and first six layer lines. Data from the micrographs of the tilt series were then combined and analyzed by a least-squares algorithm as described in detail elsewhere (6, 37) to separate terms deriving from Bessel functions of orders 0, ±3, and ±6 on each layer line. Weak terms and those in which the phase did not oscillate as expected for a sum of Bessel functions were deleted before these data were used to produce a three-dimensional reconstruction by Fourier-Bessel inversion as described by DeRosier and Moore (8). Because of the asymmetrical distribution of stain, the equator was not well recovered and so a model equator, corresponding to a filament shaft of 7 nm radius and myosin heads extending to 14 nm radius was added to the reconstructions in which a shaft was included.

RESULTS

Unidirectional Shadowing

Frog thick filaments shadowed with either platinum or platinum-carbon display a striking right-handed near-helical arrangement of subunits on their surfaces. As previously noted for other thick filaments (2, 21, 42), the appearance of the filaments is dependent on their orientation relative to the direction of shadowing because of a differential enhancement by the platinum of different aspects of the structure depending on the shadowing geometry. In filaments oriented with their long axes nearly perpendicular to the direction of shadowing, the individual subunits are not well defined, and the helical striations appear as continuous ridges of density. In filaments oriented nearly parallel to the direction of shadowing, the pattern of subunits along the filament is more completely delineated. These filaments at low magnification (Fig. 1 *a*, arrow heads) typically appear very periodic with a distinctive "double-helical" appearance resulting from periodic variations in the apparent diameter of the filament. At higher magnification, this pattern can be seen to result from a periodic arrangement of subunits on the filament surface (Figs. 1 *b–e*) along right-handed near-helical strands. These strands of subunits extend uniformly across both arms of the filament at axial intervals of ~43 nm, but are absent along the entire length of the bare zone (Fig. 1 *a–e*), consistent with the interpretation that the majority of the subunits are the myosin cross-bridges.

Measurements of the distance each strand extends axially along the filament average 60.2 ± SD 7.9 nm (n = 44), consistent with the presence of 4–5 cross-bridge levels per half turn of each strand. Although this number of subunits can be counted in some cases along the individual strands, in most cases the number cannot be ascertained because of an incomplete delineation of the subunits, possibly due in part to the presence of accessory proteins. The average diameter of the shadowed filaments (28.8 ±

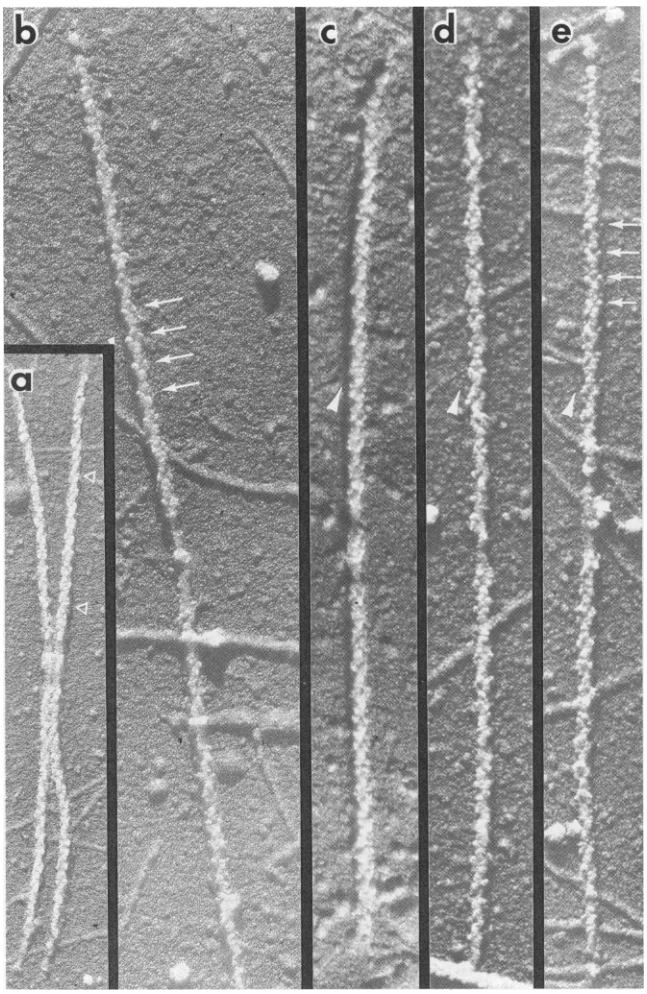

FIGURE 1 Low (*a*) and high (*b–e*) magnification electron micrographs of frog thick filaments unidirectionally shadowed with platinum. Note the periodic appearance of the filaments with subunits lying along right-handed strands which can be seen by sighting along the direction indicated by the white arrowheads in (*c–e*). The triangles in (*a*) delineate a region which shows the "double helical" appearance noted in the text. The arrows in (*b*) and (*e*) denote regions in which the 43 nm axial repeat of subunits along the filament can be seen. Magnifications: (*a*) 70,000×. (*b*) 128,000×. (*c*) 122,000×. (*d*) 116,000×. (*e*) 116,000×.

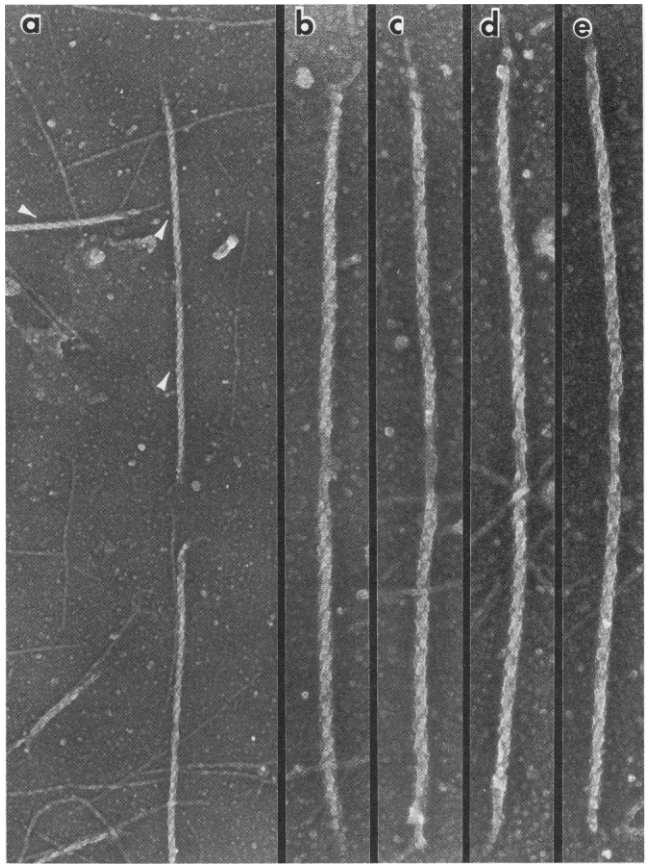

FIGURE 2 Low (*a*) and high (*b–e*) magnification electron micrograph images of frog thick filaments rotary shadowed with platinum. (*a*) shows a low magnification field in which the highly periodic appearance of the filaments can be seen. The white arrowheads in (*a*) denote regions of a filament which appear particularly periodic and show indications of the "double helical" appearance noted in the unidirectionally shadowed filaments. Figs. *b–e* show high-magnification views in which the periodicity of the filaments can be best seen by sighting along the filament axes. Note that although there is some indication of subunits along the approximately helical strands, it is not as clear as in the unidirectionally shadowed filaments. Magnifications: (*a*) 56,000×. (*b*) 108,000×. (*c–e*) 116,000×.

SD 1.6 nm) is consistent with our measurements from negatively stained preparations (23).

Rotary Shadowing

Rotary shadowed filaments also appear highly periodic with a distinct helical-like pattern extending across both arms of the filament. When lightly shadowed the filaments frequently display the "double-helical" appearance seen in the unidirectionally-shadowed filaments (Fig. 2 *a*). When more heavily shadowed, this appearance is less evident, although the filaments still appear highly periodic (Fig. 2 *e*). In general, subunits along the strands do not appear as well delineated as in the unidirectionally shadowed filaments, but an indication of their presence can be seen in the high-magnification images (Figs. 2 *b–e*). Measurements show that the helical-like strands occur axially every 43 nm, consistent with the images of the unidirectionally shadowed filaments.

Optical Diffraction Analysis of Shadowed Images

The most detailed optical diffraction patterns (Fig. 3 *a–e*) were obtained from images of unidirectionally shadowed filaments oriented with their long axes parallel to the direction of shadowing, because the individual cross-bridges were most clearly delineated along these filaments. The patterns from the rotary shadowed filaments (*f*) were usually similar. Optical diffraction patterns of these filaments show a series of layer lines indexing as orders of a 43 nm repeat, as expected from the optical diffraction studies of the negatively stained filaments (23) and from x-ray

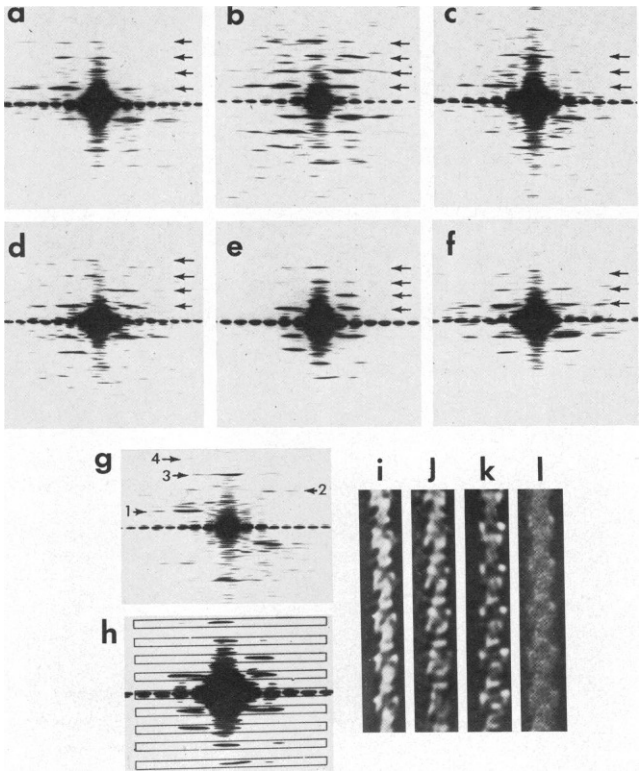

FIGURE 3 (*a–e*) shows a gallery of optical diffraction patterns obtained from unidirectionally shadowed frog thick filaments such as those shown in Fig. 1. (*f*) is from a rotary shadowed filament. The layer lines (arrows indicate their approximate position) index close to the expected spacings of a 43 nm repeat. Note the frequent occurrence of inner maxima at similar radial spacings on both sides of the meridian on the first layer line in most of the patterns, and also the frequent presence of meridional reflections on the second and fourth layer lines. These additional reflections are not expected from helical symmetry for a one-sided helical structure. Pattern (*c*) is the most typical of that expected for helical symmetry. This can be seen by comparison with (*g*) which shows a pattern obtained from a unidirectionally shadowed *Limulus* filament which has helical symmetry and shows the type of pattern one would expect to see for helical symmetry. (*h*) shows the way in which the optical diffraction patterns of the shadowed frog filaments were masked for optical filtration. As indicated, the entire layer (within the rectangular boxes) for each of the first four layer lines was allowed to contribute to the filtered image, while the areas outside of the boxes were excluded by the mask. (*i–k*) show examples of the optical filtrations obtained. Note that the filtrations show the presence of either four or five subunits per half turn of each of the nearly helical strands. Also note the presence of a repeat in the structure every third cross-bridge level (43 nm). (*l*) shows for comparison the same filament as in (*k*) averaged by photographic translational superposition (Markham translation). Note the similarity between (*k*) and (*l*).

diffraction studies of relaxed frog muscle (11, 15). The patterns typically extend to the fourth or fifth layer lines. The meridional maximum on the third layer line, which corresponds to an average axial rise of 14.3 nm between cross-bridge levels, is typically present, although variable in intensity (Fig. 3 *a–f*). Interestingly, the patterns show a marked difference from the type of pattern that would be expected from a filament with strict helical symmetry. Meridional reflections that may correspond to the "forbidden" meridional reflections seen in x-ray diffraction patterns (15) are frequently present on the second and fourth layer lines. In addition, on the first and second layer lines, inner off-meridional maxima are frequently present on both sides of the meridian at similar radial spacings (Fig. 3 *a, b, d–f*), rather than on one side as expected from simple helical symmetry. The difference between these patterns and that expected for helical symmetry can be seen by comparing patterns *a, b, d–f* to pattern *g* obtained from a shadowed *Limulus* filament, which, like the frog filaments, has a repeat every third cross-bridge level but has true helical symmetry (20, 36). This pattern (Fig. 3 *g*) shows the inner maxima on the first layer line only on the left side of the meridian and that of the second layer line only on the right side corresponding to the Bessel terms -4 and $+4$, for this filament (36). Although occasional frog filaments gave diffraction patterns (Fig. 3 *c*) similar to that expected for helical symmetry, these filaments were relatively rare, and even in these cases, the additional maxima, although weak, could usually be seen on the first layer line. Control experiments in which grids were carried through the same process except for the shadowing with platinum show very little contrast in the microscope and do not give diffraction patterns with recognizable layer lines, thus making it unlikely that the result can be caused by residual negative stain. As will be discussed, the general distribution of intensity in the optical diffraction patterns of the shadowed filaments is similar to that expected for an object with cylindrical symmetry rather than helical symmetry, and suggests a perturbation of the cross-bridge arrangement from helical symmetry.

Optical Filtration

We used optical filtration to enhance the shadowed images to make it easier to distinguish the individual cross-bridges on their surface. For the filtration, the diffraction patterns were masked to include each of the first four layer lines out to a radius of $\sim 1/7.2$ nm^{-1} on each side of the meridian (Fig. 3 *h*). No attempt was made to select only the maxima which would be expected from helical symmetry, because of the evidence that the cross-bridge array is perturbed from helical symmetry. Formally, filtration in this way was equivalent to translational superposition of the image by intervals of 43 nm. Although this procedure can be carried out in real space by photographic translation and superposition of the image on itself by multiples of the repeat spacing (Markham translation), it was generally more convenient to use optical filtering to achieve the result. Fig. 3 *i–k* illustrates the optical filtrations obtained, and for comparison, Fig. 3 *l* shows a photographic translational superposition of the same filament as in Fig. 3 *k*. The filtrations (Fig. 3 *i–k*) appear to show four to five subunits per half turn of each strand as expected for a three-stranded arrangement of subunits with a repeat every 43 nm. Simple modeling of the expected one-sided appearance

of two-, three-, and four-stranded helical arrays (data not shown) has shown that the expected number of subunits per half-turn of each helical strand is three or four for a two-stranded helix, four or five for a three-stranded helix, and six or seven for a four-stranded helix. The appearance of the shadowed filaments is thus most consistent with the expected appearance of a three-stranded arrangement of the cross-bridges, and the results support those obtained by negative staining (23). Although some of the filtrations, for example Fig. 3 *i*, appeared to show a slight deviation of the subunits from the true helical path, the resolution of the filtrations made interpretations of this type inconclusive.

NEGATIVE STAINING

Filament Appearance

To study further the structure of the filaments, we have examined filaments negatively stained with a tannic acid-uranyl acetate procedure that appeared to give higher contrast and better delineation of the cross-bridges than the uranyl acetate (alone) procedure we have previously used (23). At high magnification (Fig. 4 *a*, *b*) the filaments stained by this tannic-acid procedure display a strikingly periodic appearance which can be clearly seen by sighting along the filament axis. As previously reported (23), this cross-bridge pattern appears to have an axial repeat every third cross-bridge level (42.9 nm) and in many places (small arrows) cross-bridges can be seen projecting from the backbone at this spacing. Careful inspection of the images suggests that the cross-bridge pattern lacks the bilateral symmetry that might be expected (29) if the cross-bridges lie along an even-number of helical strands. This can be seen particularly clearly at the cross-bridge levels where the cross-bridges appear to project regularly from the filament (small arrows), while symmetrically equivalent cross-bridges do not appear to project from the other side of the filament at these levels. The appearance of the filaments is thus consistent with the cross-bridges lying along an odd-stranded structure and with our earlier evidence (23) for a three-stranded structure.

Optical Diffraction

Optical diffraction analysis of electron micrographs was used to confirm and analyze the periodicity of the filaments stained by the tannic acid-uranyl acetate procedure. Although similar to the patterns we previously described (23) for the filaments stained with uranyl acetate alone, the optical diffraction patterns from the tannic acid-uranyl acetate-stained filaments were typically stronger and often appeared to extend to a higher azimuthal resolution. The patterns (Fig. 4 *c–e*) showed a series of layer lines indexing near the expected orders of a 43 nm helical (or near helical) repeat with the expected meridional reflections on the third and sometimes sixth layer lines. Additional meridional reflections which may correspond to the "for-

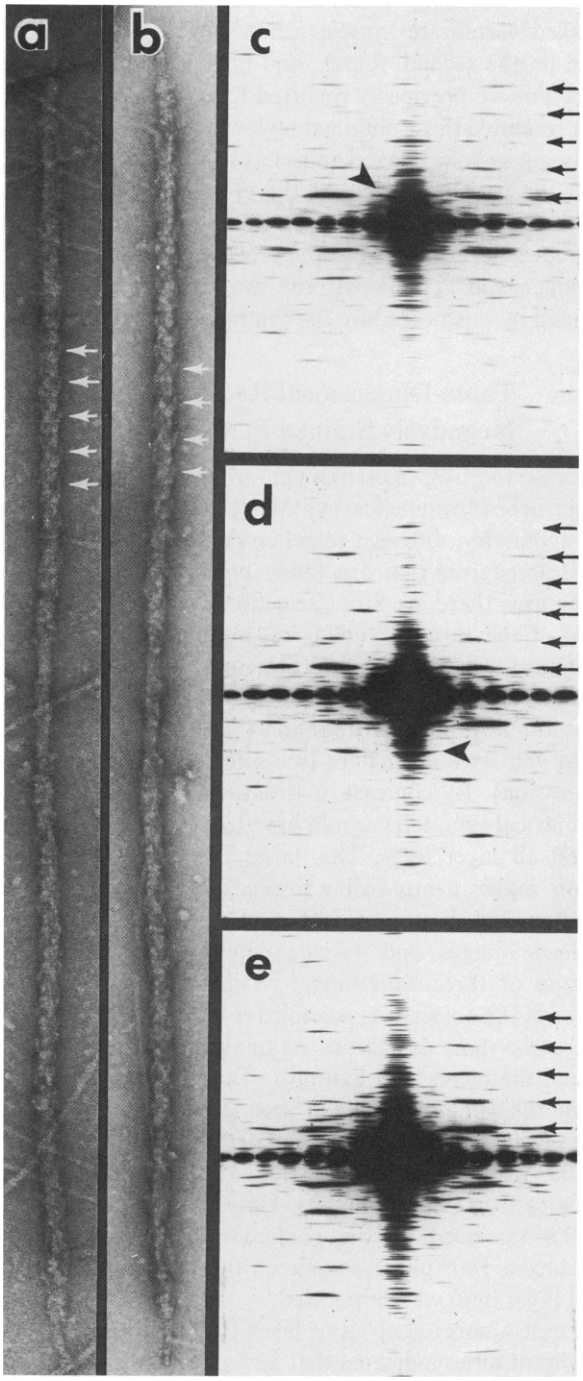

FIGURE 4 Electron micrograph images of frog filaments stained by the tannic acid-uranyl acetate negative staining procedure (*a* and *b*) and examples of optical diffraction patterns obtained from similarly stained filaments (*c–e*). Note the periodicity of the filaments, best seen by sighting along the filament axis. The white arrows point to regions where cross-bridges can be seen projecting from the filament backbone at regular intervals of 43 nm. The arrows in (*c–e*) indicate the approximate positions of the layer lines which index close to the expected orders of a 43 nm repeat in the cross-bridge array. The arrowhead in (*c*) points to what appears to be a meridional (or near meridional) reflection on the first layer line, while that in pattern (*d*) points to a similar reflection on the second layer line. Note also the presence of a meridional reflection on the fifth layer line in (*c*). Magnifications: (*a*) and (*b*) 116,000×.

bidden" meridional reflections seen in x-ray diffraction of relaxed vertebrate muscle (15, 45) were also frequently seen on the second, fourth, and fifth layer lines. Qualitatively, as we previously reported (23), the patterns generally resemble those obtained by low-angle x-ray diffraction of living, whole relaxed muscle (11, 15), thus suggesting that the native ordering of the cross-bridges had largely been preserved. Because the filaments stained by the tannic acid-uranyl acetate procedure appear to give stronger diffraction patterns we have used filaments stained by this procedure for computer-image analysis.

Three-Dimensional Reconstruction from Negatively Stained Filaments

Because the frog thick filament cross-bridge arrangement is perturbed from helical symmetry and may have cylindrical symmetry, different selection rules apply to the orders of Bessel terms that are found on layer lines. In helical structures there are strict selection rules (24), and in the case of the three-stranded frog filaments, a true helical structure would have terms deriving from Bessel orders 3 and -6 on the first and fourth layer lines; -3 and 6 on the second and fifth layer lines and 0 and ± 9 on the equator, third and sixth layer lines (see reference 32 for a detailed discussion). By contrast, a three-stranded structure with cylindrical symmetry would have terms of order 0, ± 3, ± 6, ... on all layer lines. This large number of overlapping terms makes it impossible to separate contributions from the top and bottom surfaces of (two-sided) negatively stained images and so one cannot produce one-sided images or three-dimensional reconstructions from single views of the object as is possible for most helical objects. To overcome these difficulties we analyzed tilt series of individual filaments. The azimuth of each image was known from the goniometer stage setting and this allowed the least-squares method used for arthropod thick filaments (6, 37) to be used to produce three-dimensional reconstructions of frog thick filaments. Only filaments flattened by $<20\%$ (assessed by the goniometer rotation needed to produce a 180° phase change on the inner maxima of the first layer line) were processed.

Least-squares analysis of layer line data derived from a single tilt series indicated that 82% of the intensity on layer lines one through six could be accounted for by a sum of terms deriving from Bessel terms of order 0, ± 3, and ± 6. Although this residual was not as small as observed with *Limulus* and scorpion filaments (37), it still indicated a high degree of internal consistency in the images. The separated Bessel data were used to produce the three-dimensional reconstruction of the filament shown in Fig. 5.

At a radius of 10–12 nm in the reconstruction, there were three sets of bilobed densities every 42.9 nm. The general appearance of these morphological subunits was similar to the projecting subunits seen in three-dimensional reconstructions of *Limulus* and scorpion muscle thick filaments (37) and we tentatively identified them with the nine cross-bridges expected every 43 nm axially for the three-stranded frog thick filaments (23). Although these units overlapped considerably to form almost continuous ridges of density on the filament surface, they were clearly displaced both axially and azimuthally from the positions expected in a true helical structure. There were also three lobes of density at lower radius (7 nm) arranged every 42.9 nm, which we have tentatively identified as an accessory protein such as C-protein or x-protein. We caution that our interpretation is based on a single reconstruction and so must be considered as extremely tentative until further reconstructions have been examined so that we can assess to what extent these features are reproducible.

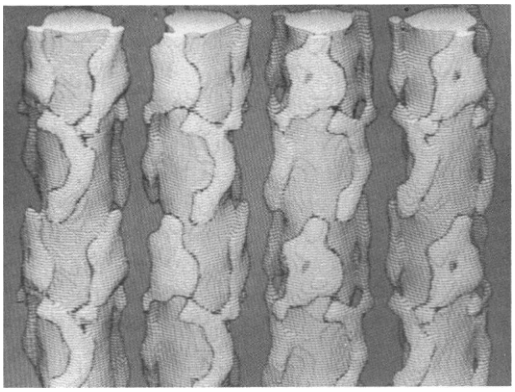

FIGURE 5 Pseudo-solid computer generated models of a three-dimensional reconstruction using separated Bessel terms on layer lines 1 through 6 from a single frog thick filament. Successive views are rotated azimuthally by 30° to enable the overall shape of the projecting morphological units to be appreciated. A model equator has been added to the layer line data to introduce a shaft of radius 7 nm into the reconstruction. Bar is 20 nm.

DISCUSSION

In a previous study (23) we provided evidence from negative staining and computer image analysis that the myosin heads in the frog thick filament are arranged along a three-stranded structure. These studies did not, however, allow a complete delineation of the individual myosin heads. In the present study, we have further examined the structure of these filaments by several approaches including a more extensive study of the filaments by platinum shadowing. Although of potentially lower resolution than negative staining, heavy metal-shadowing has the advantage that only the upper surface of the filament is contrasted, thus avoiding the superpositioning of detail from both the upper and lower surfaces which is seen with negative staining. Using both unidirectional and rotary shadowing, we have demonstrated that the filaments have a highly ordered array of subunits on their surfaces, thus extending our earlier shadowing results (23) in which we were not able to clearly delineate the arrangement of the subunits on the filament surface.

As expected from earlier x-ray diffraction studies of relaxed frog muscle (11, 15) and our previous negative staining results (23), the shadowed filaments display a repeating array of subunits arranged along virtually continuous near-helical strands on the filament surface. The subunit pattern has a repeat every 43 nm as assessed both visually and by optical diffraction of the images. Although this is most easily seen in the unidirectionally shadowed filaments, it is also apparent in the rotary shadowed images, and thus provides additional electron microscopic confirmation of this repeat distance in the vertebrate thick filament. These results differ from those of Trinick and Elliot (39), who were not able to observe the periodic order of the cross-bridges in rotary shadowed rabbit thick filaments. It is not clear to what extent this difference may depend on substrate conditions and their use of glow discharging (39) or may represent species-specific differences in the preservation of the filaments. The ability to preserve order in the cross-bridge arrangement of the frog filaments is significant in that it has allowed us to use additional techniques such as optical diffraction and optical filtration to analyze the images of the shadowed filaments.

Optical filtrations of the unidirectionally shadowed filaments show 4–5 subunits per half-turn of each strand, which is consistent with the nine myosin molecules expected to occur along a full turn of a strand in a three-stranded arrangement of the myosin cross-bridges. The presence of five subunits per half turn in some of the filtrations virtually rules out a two-stranded arrangement that would extend over a maximum of four cross-bridge levels per half turn of a strand; a four-stranded arrangement would be expected to have more subunits per turn than seen. These results, while not definitive, support our earlier evidence for a three-stranded arrangement of the cross-bridges (23) and are consistent with the results obtained by deep-etch freeze-fracture by Ip and Heuser (18) and Varriano-Marston et al. (41) for rabbit and fish thick filaments.

Perhaps the most interesting finding of the shadowing studies was the observation that the optical diffraction patterns of the images of the filaments deviate from the pattern expected for simple helical symmetry and appear consistent with cylindrical symmetry. As we noted, a three-stranded structure with cylindrical symmetry would be expected to have Bessel terms of 0, ±3, ±6, ... on all layer lines (40). This would account for both the extra meridional reflections frequently seen on the layer lines that are not multiples of three and for the additional off-meridional reflections typically seen on layer lines one and two in the patterns. Although we cannot eliminate the possibility that this perturbation of the cross-bridges from helical symmetry may be in part a preparative artifact, several lines of evidence suggest that this may not be the case. First, in x-ray diffraction patterns of vertebrate skeletal muscle thick filaments, the third and sixth layer lines appear to lack the minima that one would expect from only J_0 Bessel terms (11), thus suggesting that there may be additional terms not expected from helical symmetry along the layer lines. Additionally, there are appreciable meridional reflections on layer lines not indexing as a multiple of three; in particular these reflections are seen on the second, fifth, eighth, and eleventh layer lines (15, 45) and have been referred to as the "forbidden" meridional reflections (15). These "forbidden" meridional reflections have also been observed in optical diffraction patterns from electron micrographs of negatively stained cryosections of muscle (33) and isolated negatively stained thick filaments (23). It is unlikely that these "forbidden" reflections derive from other minor proteins of the filament, such as C-protein, because they decrease markedly in intensity when the muscle contracts (16, 45). Yagi et al. (45) and Squire et al. (33) have recently suggested that these reflections may derive from a fluctuation in the positions of the cross-bridges away from an exact axial spacing of 14.3 nm between cross-bridge levels. Thus, the $3N$-fold helical model of the cross-bridge arrangement on the vertebrate thick filament is likely to be only an approximation and the actual structure must deviate from it in some way.

Additional evidence for the three-stranded arrangement of the myosin cross-bridges on the frog thick filament and for their perturbation from helical symmetry has also been seen in the preliminary three-dimensional reconstruction shown here. The reconstruction showed bilobed features at a radius of 10–12 nm that qualitatively resembled the projecting subunits seen in *Limulus* and scorpion thick-filament reconstructions (37), which we have tentatively identified with myosin cross-bridges. Three of these subunits (presumably myosin) occurred every 14.3 nm and overlapped substantially with similar subunits at the adjacent cross-bridge levels so as to form three virtually continuous strands or ridges on the filament surface, consistent with our previous evidence (23) that the cross-bridges lie along three strands. This overlapping of the myosins probably explains the weakness of the 14.3 nm meridional reflection. Although the evidence in the reconstruction for a perturbation in the cross-bridge arrangement appears to support the shadowing results and to be consistent with the suggestion of Yagi et al. (45) and Squire et al. (33) that the cross-bridge levels may fluctuate from an exact 14.3 nm spacing, these conclusions should be considered tentative, and more detailed information about the structure of the filament must await the production of higher resolution reconstructions based on a larger number of filaments. We are presently attempting to do this by averaging data from a number of tilt series.

We wish to thank our colleagues in Philadelphia and Cambridge, particularly Rhea Levine, Hugh Huxley, and Andrew P. Somlyo, for their many helpful comments, criticisms, and suggestions. We also thank Tony Crowther, Terry Horsnell, and Judy Smith for computer programs.

This work was supported in part by U. S. Public Health Service grant AM30442 to R. W. Kensler.

Received for publication 15 May 1985 and in revised form 28 June 1985.

REFERENCE

1. Casper, D. L. D., C. Cohen, and W. Longley. 1969. Tropomyosin: crystal structure, polymorphism, and molecular interactions. *J. Mol. Biol.* 41:87.
2. Castellani, L., P. Vibert, and C. Cohen. 1983. Structure of myosin/paramyosin filaments from a molliscan smooth muscle. *J. Mol. Biol.* 167:853–872.
3. Chowrashi, P. K., and F. A. Pepe. 1977. Light meromyosin paracrystal formation. *J. Cell Biol.* 74:136–152.
4. Craig, R., and G. Offer. 1976. The location of C-protein in rabbit skeletal muscle filaments. *Proc. R. Soc. Lond. B. Biol. Sci.* 192:451–461.
5. Craig, R., and R. Padron. 1982. Structure of tarantula muscle thick filaments. *J. Muscle Res. Cell Motil.* 3:487 (Abstr.).
6. Crowther, R. A., R. Padron, and R. Craig. 1985. Three-dimensional structure of tarantula thick filaments. *J. Mol. Biol.* In press.
7. Davies, R. E. 1963. A molecular theory of muscle contractions: calcium dependent contractions with hydrogen bond formation plus ATP-dependent extensions of part of the myosin-actin cross-bridges. *Nature (Lond.)*. 199:1068–1074.
8. DeRosier, D. J., and P. B. Moore. 1971. Reconstruction of three-dimensional images from electron micrographs of structures with helical symmetry. *J. Mol. Biol.* 52:355–369.
9. Elliot, A., and G. Offer. 1978. Shape and flexibility of the myosin molecule. *J. Mol. Biol.* 123:505–519.
10. Haselgrove, J. C. 1975. X-ray evidence for conformational changes in the myosin filaments of vertebrate striated muscle. *J. Mol. Biol.* 92:113–143.
11. Haselgrove, J. C. 1980. A model of myosin cross-bridge structure consistent with the low-angle x-ray diffraction pattern of vertebrate muscle. *J. Muscle Res. Cell Motil.* 1:177–191.
12. Haselgrove, J. C., and C. D. Rodger. 1980. The interpretation of x-ray diffraction patterns from vertebrate striated muscle. *J. Muscle Res. Cell Motil.* 1:371–390.
13. Huxley, A. F., and R. Niedergerke. 1954. Structural changes in muscle during contraction. Interference microscopy of living muscle fibres. *Nature (Lond.)*. 173:971–972.
14. Huxley, H. E. 1963. Electron microscope studies of the structure of natural and synthetic protein filaments from muscle. *J. Mol. Biol.* 7:281–308.
15. Huxley, H. E., and W. Brown. 1967. The low angle x-ray diagram of vertebrate striated muscle and its behavior during contraction and rigor. *J. Mol. Biol.* 30:383–434.
16. Huxley, H. E., A. R. Faruqi, M. Kross, J. Bordas, and M. H. J. Koch. 1982. Time-resolved x-ray diffraction studies of the myosin layer-line reflections during muscle contraction. *J. Mol. Biol.* 158:637–684.
17. Huxley, H. E., and J. Hanson. 1954. Changes in the cross-striations of muscle during contraction and stretch and their structural interpretation. *Nature (Lond.)*. 173:973–976.
18. Ip, W., and J. Heuser. 1983. Direct visualization of the myosin cross-bridge lattice on relaxed rabbit psoas thick filaments. *J. Mol. Biol.* 171:105–109.
19. Kaminer, B., E. Szonyi, and C. D. Belcher. 1976. "Hybrid" myosin filaments from smooth and striated muscle. *J. Mol. Biol.* 100:379–386.
20. Kensler, R. W., and R. J. C. Levine. 1982 *a*. An electron microscope and optical diffraction analysis of the structure of *Limulus* telson muscle thick filaments. *J. Cell Biol.* 92:443–451.
21. Kensler, R. W., and R. J. C. Levine. 1982 *b*. Determination of the handedness of the cross-bridge helix of *Limulus* thick filaments. *J. Muscle Res. Cell Motil.* 3:349–361.
22. Kensler, R. W., R. J. C. Levine, and M. Stewart. 1985. An electron microscope and optical diffraction analysis of the structure of scorpion muscle thick filaments. *J. Cell Biol.* 101:395–401.
23. Kensler, R. W., and M. Stewart. 1983. Frog skeletal muscle thick filaments are three-stranded. *J. Cell Biol.* 96:1797–1802.
24. Klug, A., F. H. C. Crick, and H. W. Wykoff. 1958. Diffraction by helical structures. *Acta Crystallogr.* 11:199–213.
25. Levine, R. J. C., R. W. Kensler, M. C. Reedy, W. Hofmann, and H. A. King. 1983. Structure and paramyosin content of tarantula thick filaments. *J. Cell Biol.* 97:186–195.
26. Matsubara, I., and B. Millman. 1974. X-ray diffraction patterns from mammalian heart muscle. *J. Mol. Biol.* 82:527–536.
27. McLachlan, A. D., and J. Karn. 1983. Periodic features in the amino acid sequence of nematode myosin rod. *J. Mol. Biol.* 164:605–626.
28. Millman, B. 1979. X-ray diffraction from chicken skeletal muscle. *In* Motility in Cell Function. Proc. John M. Marshall Symp. Cell Biol. F. A. Pepe, J. W. Sanger, and V. Nachmias, editors. Academic Press, Inc., New York. 1:351–354.
29. Moody, M. F. 1967. Structure of the sheath of bacteriophage T4. I. Structure of the contracted sheath and polysheath. *J. Mol. Biol.* 25:167–200.
30. Rome, E. 1972. Relaxation of glycerinated muscles: low-angle x-ray diffraction studies. *J. Mol. Biol.* 65:331–345.
31. Safer, D., and F. A. Pepe. 1980. Axial packing in light meromyosin paracrystals. *J. Mol. Biol.* 136:343–358.
32. Squire, J. M. 1981. The structural basis of muscle contraction. Plenum Publishing Corp. Ltd., London. 225–521.
33. Squire, J. M., J. J. Harford, A. C. Edman, and M. Sjostrom. 1982. Fine structure of the A-band in cryo-sections. III. Cross-bridge distribution and the axial structure of the human C-zone. *J. Mol. Biol.* 155:467–494.
34. Starr, R., and G. Offer. 1971. Polypeptide chains of intermediate molecular weight in myosin preparations. *FEBS (Fed. Eur. Biochem. Soc.) Lett.* 15:40–44.
35. Starr, R., and G. Offer. 1983. H-protein and x-protein. Two new components of the thick filaments of vertebrate skeletal muscle. *J. Mol. Biol.* 170:675–698.
36. Stewart, M., R. W. Kensler, and R. J. C. Levine. 1981. Structure of *Limulus* telson muscle thick filaments. *J. Mol. Biol.* 153:781–790.
37. Stewart, M., R. W. Kensler, and R. J. C. Levine. 1985. Three-Dimensional reconstruction of thick filaments from *Limulus* and scorpion muscle. *J. Cell Biol.* 101:402–411.
38. Taylor, K. A., and L. A. Amos. 1981. A new model for the geometry of the binding of myosin cross-bridges to muscle thin filaments. *J. Mol. Biol.* 147:297–324.
39. Trinick, J., and A. Elliot. 1982. Effect of substrate on freeze-dried and shadowed protein structures. *J. Microscopy.* 126:151–156.
40. Vainshtein, B. K. 1966. Diffraction of X-rays by Chain Molecules. Elsevier Publ. Co., Amsterdam.
41. Varriano-Marston, E., C. Franzini-Armstrong, and J. C. Haselgrove. 1984. The structure and deposition of cross-bridges in deep-etched fish muscle. *J. Muscle Res. Cell Motil.* 5:363–386.
42. Vibert, P., and R. Craig. 1983. Electron microscopy and image analysis of myosin filaments from scallop striated muscle. *J. Mol. Biol.* 165:303–320.
43. Wray, J. 1982. Organization of myosin in invertebrate thick filaments. *In* Basic Biology of Muscle: A Comparative Approach. B. M. Twarog, R. J. C. Levine, and M. M. Dewey, editors. Raven Press, New York. 29–36.
44. Wrigley, N. G. 1968. The lattice spacing of crystalline catalase as an internal standard of length in electron microscopy. *J. Ultrastruc. Res.* 24:454–464.
45. Yagi, W., E. J. O'Brien, and I. Matsubara. 1981. Changes of thick filament structure during contraction of frog striated muscle. *Biophys. J.* 33:121–138.

DISCUSSION

Discussion Chairman: Thomas D. Pollard
Scribes: Piotr Fajer, Eric Baldwin, and Vincent Barnett, with special thanks to Murray Stewart

MAKOWSKI: Were your filaments unidirectionally shadowed?

KENSLER: Yes, but rotary shadowing gives similar results.

MAKOWSKI: What was the shadowing direction?

KENSLER: It was along the filament axis.

MAKOWSKI: If you shadowed from other directions you might have extra Bessel terms on layer lines giving additional reflections without having a perturbation of heads.

KENSLER: In shadowed material some parts of the structure can be preferentially enhanced. However, we have rotary shadowed patterns that are similar to unidirectional ones. Furthermore, patterns from unidirectionally shadowed helical Arthropod filaments showed the expected one-sided pattern (see Fig. 3*g*).

RUBEN: Are your rotary shadowed patterns as well preserved as the unidirectionally shadowed ones?

KENSLER: Yes.

RUBEN: We find unidirectional shadowing is better at high resolution.

KENSLER: With a light rotary shadowing we seem to have preserved structure. However, rotary shadowed material does not appear to have intrinsically high resolution detail.

SHARNOFF: Did your filaments contain only myosin?

KENSLER: They probably had some accessory protein as well, because we see stripes at 43 nm intervals in isolated A-segments similar to those seen in rabbit and ascribed to C-protein (see reference 4).

LYMN: Should you describe the structure as cylindrically symmetrical, or say it is a distorted helix?

STEWART: Helical symmetry is a special case of cylindrical symmetry. In the latter case the object's symmetry is characterized by a translation of 43 nm and a rotation of 120° whereas a helical object has a translation of 14.3 nm paired with a rotation of 40°. In a special case of a helix, many of the Bessel terms characteristic of cylindrical symmetry are forbidden, and the pattern becomes much simpler. Because these forbidden terms are present in our diffraction patterns, the filament should be analysed assuming cylindrical symmetry.

POLLARD: Is this arrangement peculiar to frogs or is it found in all vertebrates?

STEWART: I suspect this arrangement occurs more generally than in frogs alone. Squire (see reference 33) has seen axial perturbations in human muscle.

POLLARD: One of your reviewers complained that your filaments were too well organized. X-ray studies indicate that many of the heads may be mobile.

STEWART: There are several aspects to this. Either whole heads or only portions may be mobile. Our analysis concentrated on regions near the bare zone, and here most heads seem to be ordered. We would not see highly mobile heads in our analysis, but I do not think this presents major problem in interpreting our results since we are concentrating on the arrangement of heads rather than the detailed shape.

KENSLER: In addition, work employing etching of rapidly frozen material gives results qualitatively similar to our own (see reference 18).

TAYLOR: Does cylindrical symmetry impose restrictions on the way myosin heads can interact with actin?

KENSLER: Probably not, but it will have to be examined in future.

STEWART: The perturbation may arise because it may not be possible to pack the heads regularly or it may reflect an underlying nonhelical packing of the tails in the thick filament shaft. Thus it may not be directly related to actomyosin interaction.